

Cohesion without cooperation: the outcome of microbial community coalescence is predicted by a community-level fitness function

Mikhail Tikhonov*

Center of Mathematical Sciences and Applications

Harvard John A. Paulson School of Engineering and Applied Sciences and

Kavli Institute for Bionano Science and Technology, Harvard University, Cambridge, MA 02138, USA

Recent work draws attention to community-community encounters (“community coalescence”) as a frequent natural occurrence and an important factor shaping community structure. This work investigates such community-level competition in a minimal theoretical setting. Specifically, it builds on MacArthur’s model of competitive coexistence on multiple resources to construct a simple adaptive dynamics model for co-evolution in multi-species communities. It is shown that the likelihood of a species to survive a coalescence event is best predicted by a community-level “fitness” of its parent community rather than the intrinsic fitness of the species itself. Within the model presented here, the metaphor of a community as a coherent whole becomes mathematically exact. Importantly, this cohesion is shown to arise in a purely competitive setting as a generic consequence of division of labor, and requires no cooperative interactions. As a result, it is not vulnerable to “cheaters” and can be expected to be widespread in microbial ecosystems.

Microbial communities do not just exchange members: events of biotic and abiotic nature move pieces of the environment and cause entire communities of organisms to routinely come in contact or interchange. Recent work (Rillig *et al.* 2015) argues that such “community coalescence” events may be a major factor shaping community structure in natural microbial ecosystems, but a theoretical understanding of their ecological and evolutionary significance is lacking. Have organisms evolved specific adaptations to frequent coalescent events? Will members of communities with a history of coalescence have a higher persistence upon interaction with a “naïve” community that had never experienced such events? (Rillig *et al.* 2015)

Intriguingly, the “community coalescence” perspective naturally places emphasis on community-level interactions. Whether or not a particular species will survive a coalescence event is determined not only by its own traits and fitness, but also by the traits and fitnesses of partner species on which it depends or with which it interacts (Davis *et al.* 1998; McGill *et al.* 2006; McIntire & Fajardo 2014). Rillig *et al.* observe that in certain circumstances, the coalescing communities appear to be “interacting as internally integrated units rather than as a collection of species that suddenly interact with another collection of species” (Rillig *et al.* 2015). Some recent results allowing such interpretation include the observed efficacy of fecal transplant in treating *C. difficile* infections (Bakken *et al.* 2011) or “lean microbiota” outcompeting “obese microbiota” in mice (Ridaura *et al.* 2013).

Whether natural microbial communities could be thought of as integrated units, and perhaps even multicellular organisms is a recurring theme in the ecological literature (Shapiro 1998, West *et al.* 2006). Most commonly, discussions of such coherence focus on adaptive

costs and benefits of various forms of intra- or inter-species cooperation. This work pursues two goals: First, present a theoretical framework where the metaphor of a community as a coherent whole becomes an exact mathematical statement. Second, demonstrate that internal coherence is conceptually separate from discussions of cooperation and loaded terms such as “cheating” and “altruism”.

Specifically, building on MacArthur’s model of competitive coexistence on multiple resources (MacArthur, 1969), this work constructs a simple adaptive dynamics framework that describes co-evolution in multi-species communities (Roughgarden 1976; Geritz *et al.* 1998; Nurmi & Parvinen 2008). This model allows investigating the coalescence phenomenon in a minimal theoretical setting. It is shown that, surprisingly, the likelihood of a species to survive a coalescence event is best predicted by a community-level function characterizing the community of which it was part, rather than by the intrinsic fitness of the species itself. When coalescence events are interpreted as competition between communities, this function is shown to act as “community fitness” that predicts competitive success of a co-evolved community.

Importantly, all results are derived in a purely competitive setting, with no cooperative interactions or relatedness typically associated with emergence of functional integration or “collective traits” (e.g. Queller 2000; Okasha 2008; Queller & Strassmann 2009; Levin *et al.* 2015). If largely isolated populations interact through coalescence events, internal coherence can arise simply as a consequence of this externally imposed population structure. Similar ideas were explored by Slatkin and Wilson (Wilson 1977; Slatkin & Wilson 1979) who noted that the outcome of co-evolution in structured demes depends on how individuals are exchanged between groups. Here it is proposed that if wholesale community exchange events are indeed a frequent occurrence in nature, then communities “acting as a coherent whole”, in a rigorous mathematical, rather than purely metaphorical, sense, can be

* tikhonov@fas.harvard.edu

expected to be ubiquitous in microbial ecology.

I. THE METAGENOME PARTITIONING MODEL

To investigate community coalescence in the simplest theoretical setting, consider the following model for division of labor in large communities. It is closely related to MacArthur’s model of competitive coexistence on multiple resources (MacArthur 1969); see Supplementary Material (SM).

Consider a community in a habitat where a single limiting resource exists in N forms (“substrates” $i \in \{1 \dots N\}$) denoted A, B , etc. For example, this could be carbon-limited growth in an environment with N carbon sources, or a community limited by availability of electron acceptors in an environment with N oxidants. The substrates can be utilized with “pathways” P_i (one specialized pathway per substrate). A species is defined by the pathways that it carries (similar, for example, to the approach of Levin *et al.* 1990). There is a total of $2^N - 1$ possible species in this model; they will be denoted using a binary vector of pathway presence/absence: $\vec{\sigma} = \{1, 1, 0, 1, \dots\}$, or by a string listing all substrates they can use, e.g. “species ABD” (the underline distinguishes specialist organisms such as A from the substrate they consume, in this case A). Let $n_{\vec{\sigma}}$ be the total abundance of species $\vec{\sigma}$ in the community, and let T_i be the total number of individuals capable of utilizing substrate i (Fig. 1):

$$T_i \equiv \sum_{\text{all } \vec{\sigma} \text{ carrying } i} n_{\vec{\sigma}} = \sum_{\vec{\sigma}} n_{\vec{\sigma}} \sigma_i.$$

Assume a well-mixed environment, so that each of these T_i individuals gets an equal share R_i/T_i of the total benefit R_i (carbon content, oxidation power; etc.) available from substrate i (“scramble competition”). Any one substrate is capable of sustaining growth, but accessing multiple cumulates the benefits. The population growth/death rate of species $\vec{\sigma}$ will be determined by the *resource surplus* Δ experienced by each of its individuals:

$$\Delta_{\vec{\sigma}} = \sum_i \sigma_i \frac{R_i}{T_i} - \chi_{\vec{\sigma}}. \quad (1)$$

Here the first term is the benefit harvested by all carried pathways, and the second represents the maintenance costs of organism $\vec{\sigma}$. These costs summarize all the biochemistry that makes different species more or less efficient at processing their resources. For simplicity, let these costs be random:

$$\chi_{\vec{\sigma}} = \chi_0 |\vec{\sigma}| (1 + \epsilon \xi_{\vec{\sigma}}). \quad (2)$$

Here χ_0 is a constant (the average cost per pathway), $\xi_{\vec{\sigma}}$ is a random variable drawn out of the standard normal distribution (chosen once for each species), ϵ sets the

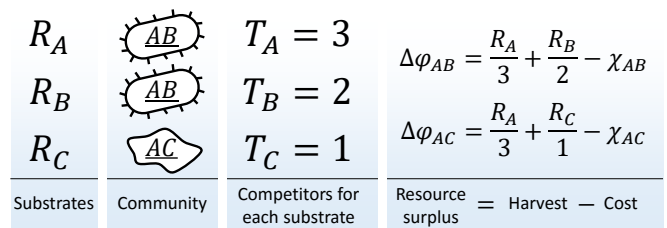


FIG. 1. **The metagenome partitioning model.** Organisms are defined by the pathways they carry, the benefit from each substrate is equally partitioned among all organisms who can use it, and population growth/death of each species is determined by the resource surplus it experiences.

magnitude of cost fluctuations, and $|\vec{\sigma}| \equiv \sum_i \sigma_i$ is the number of pathways carried by the species. The reason for including this factor will become clear shortly.

The resource surplus Δ is used to generate biomass. The simplest approach is to equate the biomass of an organism with its cost, so that the total biomass of a species is $\chi_{\vec{\sigma}} n_{\vec{\sigma}}$, and the dynamics of the model are given by:

$$\tau_0 \chi_{\vec{\sigma}} \frac{dn_{\vec{\sigma}}}{dt} \equiv g_{\vec{\sigma}}(\{n_{\vec{\sigma}}\}) = n_{\vec{\sigma}} \Delta_{\vec{\sigma}}. \quad (3)$$

The constants χ_0 and τ_0 set the units of resource and time.

The approach taken here purposefully ignores multiple factors, most notably trophic interactions or any other form of cross-organism dependence. This is intentional: it ensures that the interaction matrix

$$M_{ab} \equiv \frac{\partial g_{\vec{\sigma}_a}}{\partial n_{\vec{\sigma}_b}}$$

has no positive terms, i.e. the setting is purely competitive (indices a, b label species). This helps underline that the whole-community behavior exhibited below is a generic consequence of division of labor, and requires no explicitly cooperative interactions.

Other simplifications include the assumption of deterministic dynamics and a well-mixed environment. Although stochasticity and spatial structure are tremendously important in most contexts, the simplified model adopted here provides a convenient starting point and makes the problem tractable analytically.

This work will investigate coalescence of communities that originate and remain in similar environments, e.g., transfer of oral communities by kissing (Kort *et al.* 2014) as opposed to invasion of microbes from the mouth into the gut (Qin *et al.* 2014). Imagine a collection of islands (or patches) labeled by α , each harboring a community \mathcal{C}_α experiencing the same environment \mathcal{E} . The next section investigates the within-island dynamics (3) to establish some key properties that make this simplified model particularly convenient for our purposes. Specifically, let $\Omega(\mathcal{C})$ denote the set of species present at non-zero abundance in a community \mathcal{C} . It will be shown that

under the dynamics (3), any community \mathcal{C} will eventually converge to a stable equilibrium \mathcal{C}^* uniquely determined by the set $\Omega(\mathcal{C})$. Here and below, the starred quantities refer to equilibrium of ecological dynamics. At this equilibrium, certain species $S^* = \Omega(\mathcal{C}^*)$ establish at a non-zero abundance, while others “go extinct”, exponentially decreasing towards zero. Importantly, the set of survivors will depend only on the identity of the initially present species, and not on their initial abundance. Thus a community \mathcal{C}_1 coalescing with \mathcal{C}_2 will yield the same community \mathcal{C}_{12}^* irrespective of the initial mixing ratios. While obviously a simplification, this makes the metagenome partitioning model an especially convenient starting point to build theoretical intuition about community-community interactions before more general situations can be studied in simulations.

These properties are established in the next section; the following section then turns to the main subject of this work, namely coalescence events between islands.

II. SINGLE-ISLAND ADAPTIVE DYNAMICS: INTRINSIC FITNESS AND A COMMUNITY-LEVEL OBJECTIVE FUNCTION

Numerical simulation of the competition between all 1023 possible species, initialized at equal abundance, for $N = 10$, $\epsilon = 10^{-3}$, $R_i = 100\chi_0$, and one random realization of organism costs results in an equilibrium state depicted in Fig. 2A. In this example it consists of 9 species. It is natural to ask: for a given initial set of competitors, what determines the success of a species? Can we construct a species fitness ranking that would predict the survivors?

To define fitness, consider an assay whereby a single individual of species $\bar{\sigma}$ is placed in environment with no other organisms present, and, for simplicity, all substrates supplied in equal abundance $R_i = R$. The initial population growth rate in this chemostat is given by:

$$\left. \frac{dn_{\bar{\sigma}}}{dt} \right|_{t=0} = \frac{1}{\tau_0\chi_{\bar{\sigma}}} \left[\sum_i R_i\sigma_i - \chi_{\bar{\sigma}} \right] = \frac{1}{\tau_0} \left[R \frac{|\bar{\sigma}|}{\chi_{\bar{\sigma}}} - 1 \right]$$

and abundance eventually equilibrates at $n_{\bar{\sigma}} = R|\bar{\sigma}|/\chi_{\bar{\sigma}}$. Both these quantities characterize fitness of species $\bar{\sigma}$, and are determined by its cost per pathway. Throughout this work, the term “fitness” will be used in a restricted sense of a quantity predicting success at competition; in particular, here we seek to define a fitness ranking rather than absolute fitness such as the number of progeny. For this purpose, additive constants and rescaling are irrelevant, and we can define the intrinsic fitness of $\bar{\sigma}$ as

$$f_{\bar{\sigma}} \equiv \frac{|\bar{\sigma}|\chi_0}{\chi_{\bar{\sigma}}} - 1. \quad (4)$$

This definition is convenient as it makes $f_{\bar{\sigma}}$ a dimensionless quantity of order ϵ . Under the cost model (2), the

fitness ranking between species is random, set by the random realization of the costs ξ .

Fig. 2 demonstrates that the intrinsic fitness defined in this way is a fairly good predictor of the outcome of within-community competition. Indeed, the equilibrium depicted in panel A includes the top 3 fittest species, and the remaining are all within the top 30 (out of 1023). To confirm the generality of this observation, 100 randomly initialized populations were equilibrated, for a range of ϵ (see SM for the exact protocol). For each ϵ , Fig. 2B shows the median fitness rank of survivors, averaged over all 100 instances, where the median was either weighted (blue dashed line) or not weighted (red solid line) by abundance of the species at equilibrium. Note that for small ϵ , the structure of the final equilibria does not significantly depend on this parameter (see SM). In what follows, ϵ will be fixed at $10^{-3} \approx 2^{-N}$, and the large- ϵ regime will be discussed later. For all ϵ , the median rank of survivors is low, and weighted median is lower still, indicating that fitter species tend to be present at higher abundance (Davis *et al.* 1998; Birch 1953). This figure confirms that the fitness rank of a species is strongly correlated both with its probability of survival and with its abundance at equilibrium.

This is intuitive: $\chi_{\bar{\sigma}}$ is the lowest resource harvest at which an organism can persist, and by analogy with Tilman’s R^* rule (Tilman 1990), low-cost species should have a competitive advantage. However, Fig. 2 also demonstrates that this notion of intrinsic fitness is not wholly sufficient. For example, at the equilibrium shown in Fig. 2A, the species ranked 4th in fitness went extinct, but 6 others ranked as low as #29 remained present, despite being intrinsically “less fit”.

The origin of this is very general and lies, of course,

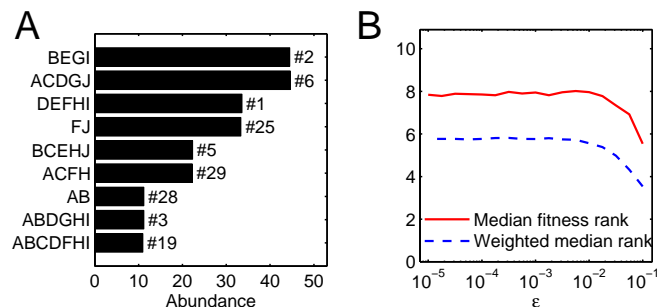


FIG. 2. **Intrinsic fitness of a species is predictive of both its survival and abundance at equilibrium.** **A:** Community equilibrium for one particular random realization of the model ($N = 10$, $\epsilon = 10^{-3}$). Species are ordered by abundance and labeled by the pathways they carry. Also indicated is the fitness rank; all surviving species were within the top 30 by intrinsic fitness (out of 1023). **B:** The median fitness rank of survivors, weighted (dashed) or not weighted (solid) by abundance. Curves show mean over 100 random communities for each ϵ ; the standard deviation across 100 instances is stable at approximately 40% of the mean for both curves, independently of ϵ (not shown to reduce clutter).

in the context-dependent nature of fitness. As organisms reproduce or die, they modify their environment (interaction milieu; McGill *et al.* 2006) and thus their own fitness and the fitness of all other species (McIntire & Fajardo 2014). Conveniently, in the model described here, these complex effects studied by niche construction theory can be summarized in a single community-level objective function. The dynamics (3) possess a Lyapunov function (compare to MacArthur 1969):

$$F = \frac{1}{R_{\text{tot}}} \left(\sum_i R_i \ln \frac{T_i}{R_i/\chi_0} - \sum_{\bar{\sigma}} \chi_{\bar{\sigma}} n_{\bar{\sigma}} + R_{\text{tot}} \right). \quad (5)$$

Here R_{tot} is a constant introduced for later convenience. Specifically, set $R_{\text{tot}} = \sum_i R_i$; this choice ensures that close to community equilibrium, F is also of order ϵ (see SM). This function, defined for $n_{\bar{\sigma}} \geq 0$ and $T_i > 0$, has the property that $R_{\text{tot}} \frac{\partial F}{\partial n_{\bar{\sigma}}} = \Delta_{\bar{\sigma}}$, and therefore

$$\frac{dF}{dt} = \sum_{\bar{\sigma}} \frac{\partial F}{\partial n_{\bar{\sigma}}} \frac{dn_{\bar{\sigma}}}{dt} = \sum_{\bar{\sigma}} \frac{n_{\bar{\sigma}} (\Delta_{\bar{\sigma}})^2}{R_{\text{tot}} \chi_0 \tau_0} > 0$$

Thus F is monotonically increasing as the system is converging to equilibrium. To illustrate this, Fig. 3 shows 10 trajectories of ecological dynamics for the same system as in Fig. 2A, starting from random initial conditions (with all species present; see SM). Far from equilibrium, mean intrinsic fitness of members and F increase together (Fig. 3, inset), confirming that intrinsic fitness is a useful predictor. However, as the equilibrium is approached, Fig. 3 shows that virtually every trajectory has portions whereby dynamics increase F at the expense of the naïve mean fitness of individual community members. The following sections will argue that F can be thought of as community-level “fitness”, but this term will not be used until justification is provided.

Each of the trajectories in Fig. 3 converges to the same equilibrium (depicted in Fig. 2A). This is because F is convex and bounded from above (see SM). Therefore, for every set of species Ω , any community restricted to these species will always reach the same (stable) equilibrium, corresponding to the unique maximum of F on the subspace V_{Ω} defined by the conditions $\{n_{\bar{\sigma}} = 0 \text{ for all } \bar{\sigma} \notin \Omega\}$. This maximum will often be at the border of this subspace, corresponding to the extinction of some species.

Under the dynamics (3), no new species can “appear” if their original abundance was zero. Imagine, however, that on each island, a rare mutation occasionally introduces a random new species; if it can invade, the community transitions to a new equilibrium and awaits a new mutation. This process of adaptive dynamics defines the evolution of each island, and can be seen as a mesoscopic population genetics model for a multi-species community evolving through horizontal gene transfer (loss/acquisition of whole pathways). Importantly, for each island, F is monotonically increasing throughout its evolution. Indeed, F is continuous and non-singular in

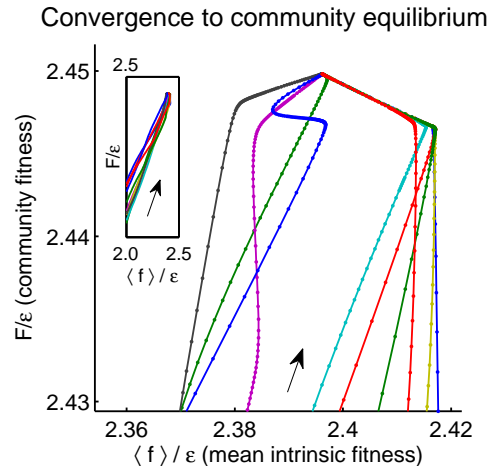


FIG. 3. **Community dynamics maximize a global objective function F at the expense of mean intrinsic fitness.** 10 trajectories of ecological dynamics for an example system, starting from random initial conditions and converging to the equilibrium depicted in Fig. 2A. **Inset:** a zoomed-out version of the same plot; data aspect ratio as in the main panel. Mean intrinsic fitness is weighted by species abundance. Direction of dynamics indicated by arrows.

all $n_{\bar{\sigma}}$. Therefore, introducing a new species at a vanishingly small abundance will leave F unchanged, and if it can invade the community, the convergence to the new equilibrium is a valid trajectory of ecological dynamics on which F increases.

III. THE OUTCOME OF COMMUNITY COALESCENCE IS BEST PREDICTED BY THE COMMUNITY-LEVEL FUNCTION F

Consider now a coalescence event whereby the equilibrium communities from two islands \mathcal{C}_{α}^* and \mathcal{C}_{β}^* are brought into contact; as established above, the resulting community \mathcal{C}^* will not depend on the details of the mixing protocol. If none of the species from island β could invade the community \mathcal{C}_{α}^* , then $\mathcal{C}^* = \mathcal{C}_{\alpha}^*$ and the community \mathcal{C}_{α}^* is the clear winner. In general, however, the space of competition outcomes is richer than merely one community taking over: both competitors \mathcal{C}_{α}^* , \mathcal{C}_{β}^* can contribute to \mathcal{C}^* , but can be more or less successful at doing so, contributing more or fewer species. What makes a community more likely to be successful?

Let \mathcal{C}_{α}^* and \mathcal{C}_{β}^* each consist of k species. On the one hand, the community \mathcal{C}^* is simply the result of competition between $2k$ species (fewer if $\Omega(\mathcal{C}_{\alpha}^*)$ and $\Omega(\mathcal{C}_{\beta}^*)$ overlap), and we have established (Fig. 2) that the individual fitness rank of a species is a good predictor of its survival. One may therefore expect that the community whose members have higher average intrinsic fitness should be more successful. On the other hand, we also found that the ultimate equilibrium community that can-

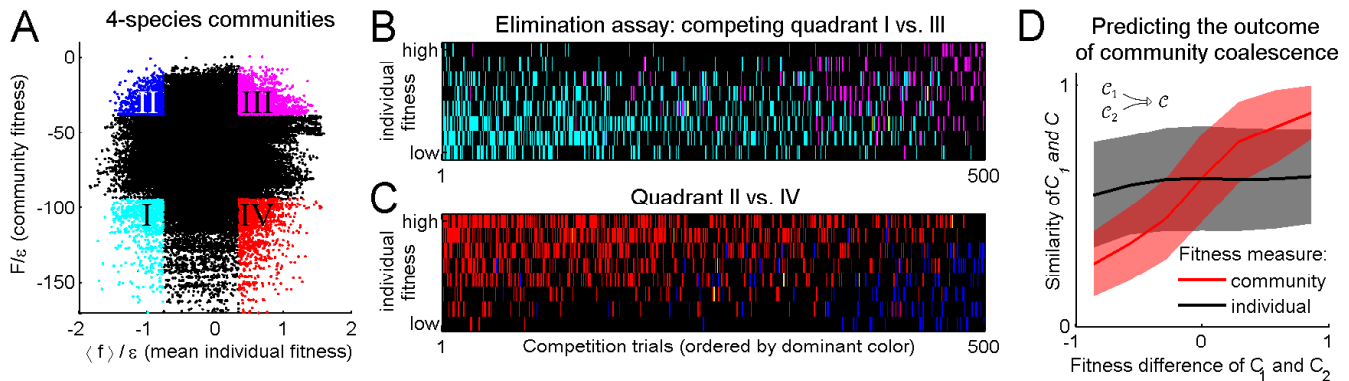


FIG. 4. Community fitness is more predictive of competition outcome than intrinsic fitness of individuals. **A:** Community fitness *vs.* mean intrinsic fitness, measured in units of ϵ , for 70160 communities composed of 4 species (see text). Communities in which both characteristics are in the top 10% or bottom 10% are highlighted in color and labeled I through IV. **B:** Elimination assay competing quadrants I (cyan) vs III (magenta). 500 randomly drawn community pairs (columns) were jointly equilibrated, with up to 8 species each time (rows; ordered by intrinsic fitness). For each species that went extinct during equilibration, the corresponding cell in the table is colored by the species’ provenance. As expected, most eliminated species were from the less fit cyan communities (there are more cyan cells than magenta). These species were also less fit intrinsically (most colored cells are in the lower half of the table). **C:** Same, competing quadrants II (blue) vs IV (red). The dominant color is now red: most eliminated species were from red communities, and went extinct despite being intrinsically more fit than average (most colored cells are in the upper half of the table). Columns ordered by dominant color. **D:** Community similarity $S(C_1, C)$ for a coalescence event depicted in the cartoon (inset), computed for 5000 random community pairs, as a function of fitness difference between competing communities. Fitness difference scaled to the maximum of 1 so both fitness measures can be shown in same axes. Shown is binned mean (8 bins) over communities with similar fitness difference (solid line) ± 1 standard deviation (shaded region).

not be invaded by *any* species corresponds to the global maximum of F , and not of the mean intrinsic fitness. This suggests that the community-level function F could be the better predictor of the competition outcome. If so, it could be said to characterize the “collective fitness” of a community, as opposed to the “individual” intrinsic fitness of community members; again, it should be stressed that the term “fitness” is used in the restricted, purely competitive, rather than reproductive, sense.

To settle the competition between these two hypotheses, the following procedure was implemented. For $N = 10$, $\epsilon = 10^{-3}$, and a given random realization of the cost structure ξ , $M = 50$ random species were selected to allow for an exhaustive sampling of sub-communities; the results reported below do not significantly depend on this choice. This set was used to construct all $\binom{50}{4} = 230300$ possible combinations of $k = 4$ species that were independently equilibrated; instances where the equilibrium state had fewer than $k = 4$ species or where some pathways were not represented were excluded. The mean individual fitness and the putative collective fitness F of the remaining 70160 communities are shown in Fig. 4A. This procedure puts at our disposal multiple examples of communities where individual and collective fitness are both high, both low, or one is high while the other is low (the quadrants highlighted in Fig. 4A). Competing pairs of communities drawn from these pools will make it possible to determine which of the two factors, individual or collective fitness, is the better predictor of community

competition outcome.

To begin, consider the cyan and magenta quadrants (I and III, respectively). Communities from the magenta quadrant are predicted to be more fit, both in the collective sense and as measured by the average intrinsic fitness of members. Therefore, one expects that the magenta (III) communities should, on average, be more successful in pairwise competitions. To confirm this, Fig. 4B presents the results of an “elimination assay” competing communities from these quadrants. 500 random pairs were drawn, and correspond to columns in Fig. 4B. For each pair, species from both communities (up to 8 each time, fewer if the two sets of 4 overlapped) were equilibrated together; the rows in Fig. 4B correspond to these species, ordered by individual fitness: high (top) to low (bottom). For each species that went extinct during equilibration, its provenance was identified (“did it come from the magenta or the cyan community?”), and the corresponding rectangle in Fig. 4B was colored accordingly; in the rare cases when the eliminated species was originally present in both communities, it was colored yellow. The dominant color in Fig. 4B is cyan, confirming that the cyan communities are typically less successful at contributing their members to the final equilibrium. Note also that the colored entries are predominantly located in the bottom half of the table: the eliminated species tend to also have lower individual fitness than their more successful competitors. This is the expected result.

Now, consider the competition between blue and red

quadrants (II and IV). An elimination assay conducted in an identical manner is presented in Fig. 4C. Now the colored entries are predominantly red and occupy the *top* half of the table. In other words, members of the red communities are being outcompeted despite the fact that their intrinsic fitness is higher. Surprisingly, the individual fitness of a species is less predictive of its ability to survive coalescence than the collective fitness of the community of which it was part.

Finally, 5000 random community pairs from the pool of Fig. 4A (not restricted to any quadrant) were competed. Define community similarity for $\mathcal{C}_1 \equiv \{n_{1\bar{\sigma}}\}$ and $\mathcal{C}_2 \equiv \{n_{2\bar{\sigma}}\}$ as the normalized scalar product of their species abundance vectors:

$$S(\mathcal{C}_1, \mathcal{C}_2) = \frac{\sum_{\bar{\sigma}} n_{1\bar{\sigma}} n_{2\bar{\sigma}}}{\sqrt{\sum_{\bar{\sigma}} n_{1\bar{\sigma}}^2} \sqrt{\sum_{\bar{\sigma}} n_{2\bar{\sigma}}^2}}.$$

For each of the 5000 coalescence instances $\mathcal{C}_1^* + \mathcal{C}_2^* \mapsto \mathcal{C}^*$, Fig. 4D plots the similarity $S_1 \equiv S(\mathcal{C}_1^*, \mathcal{C}^*)$ as a function of fitness difference between “parent” communities \mathcal{C}_1^* and \mathcal{C}_2^* . We see that the larger the difference in community fitness, the stronger the similarity between the post-coalescence community and its more fit parent (red line). In contrast, mean individual fitness is not predictive of the coalescence outcome (black line).

IV. THE “COMMUNITY AS AN INDIVIDUAL” METAPHOR BECOMES EXACT

Consider an observer who is unaware of the internal structure of the community on each island, and who is able to perform only “metagenomic” experiments measuring the total pathway expression $\vec{T} = \{T_i\}$ as a function of the resource influx $\vec{R} = \{R_i\}$. First, consider an island α_G harboring a single species: the complete generalist $\vec{\sigma}_G = \{1, 1, \dots, 1\}$. Its abundance at equilibrium will be $n_G = T_i = R_{\text{tot}}/\chi_G$. Although substrates may be supplied in varying abundance, the island α_G can only express all pathways at the same level.

Another island α_S might harbor a community of perfect specialists: $\underline{A} = \{1, 0, 0, \dots\}$, $\underline{B} = \{0, 1, 0, \dots\}$, etc. Faced with an uneven supply of substrates, this island will adjust expression levels T_i to precisely track the supply vector R_i , so that $T_i = R_i/\chi_i$, where χ_i is the cost of the respective specialist. Our external observer will conclude that island α_S is able to sense its environment and up-regulate or down-regulate individual pathways.

Such perfect regulation is, however, costly: typically, \underline{A} , \underline{B} , etc. will not be the most cost-efficient combinations. As a result, allowing the community to evolve while holding \vec{R} fixed, one will obtain a different multi-organism community \mathcal{C} . Unlike α_S , it will generally be unable to sense each substrate independently: evolution will trade some of the sensing capacity to fit the particular substrate influx \vec{R} with more efficient pathway combinations.

To an external observer, therefore, the community on each island is a coherent whole with an evolving complex behavior striving to better adjust its response \vec{T} to the environment \vec{R} it experiences, and in this particular model, the metaphor is rendered exact by the existence of a function F satisfying the properties of a valid fitness function: F increases throughout the evolutionary history of each island, and is predictive of its success at competition events with other islands. Importantly, however, the inner regulatory logic of this “coherent whole” has the form of purely “selfish” competition between different motifs of pathway co-expression. This invites a parallel with other instances of “competition serving the good of the multicellular whole” (Moreno & Rhiner 2014), but more importantly, the purely competitive model used here clearly shows that cohesion of a co-evolved community is conceptually separate from the discussions of “altruism” and cooperation, except to the extent described by the formula “enemy of my enemy is my friend”. The latter can be seen as a form of cooperation (Hay *et al.* 2004), but is a generic phenomenon and is not vulnerable to “cheaters”.

In the model presented here, the analogy between a community harboring organisms at varying abundances, and an organism expressing genes at different levels, becomes an exact mathematical statement. A striking feature of this perspective is the blurred boundary between the notions of competition and genetic recombination (Shapiro *et al.* 2012; Rosen *et al.* 2015). In sexual reproduction, recombination allows a subset of the genes inherited from both parents to form progeny with potentially higher fitness; here, the competition between parent communities \mathcal{C}_α^* and \mathcal{C}_β^* allows a subset of their members to regroup into a daughter community \mathcal{C}^* with a higher collective fitness F . The parallel becomes especially clear if one imagines propagules of \mathcal{C}_α^* and \mathcal{C}_β^* co-colonizing a fresh environmental patch. Member regrouping can be much more flexible than the rules of sexual recombination, but reduces to the latter in the particular case of communities with clearly demarcated functional guilds (e.g. consider competition between communities that each has one plant, one pollinator, one herbivore, one carnivore...).

To conclude this section, let us compute the community fitness F of the single-species community α_G for the case $R_i \equiv R$. Applying the definition (5), and using $T_i = n_G = NR/\chi_G$ one finds:

$$\begin{aligned} F &= \frac{1}{\sum_i R_i} \left(\sum_i R_i \ln \frac{T_i}{R_i/\chi_0} - n_G \chi_G \right) + 1 \\ &= \ln \frac{N\chi_0}{\chi_G} = \ln(1 + f_G) \approx f_G \end{aligned}$$

where f_G is the individual fitness (4) of organism σ_G , and the approximate equality holds because f_G is of order ϵ . In other words, for a single-species community, the community fitness coincides with the individual fitness of

this species, reinforcing the interpretation of a community as a “smarter” individual that had evolved internal division of labor. This interpretation is specific to the particular model explored here, but within this model, the metaphor is exact.

V. FITNESS DECOUPLING AS A GENERIC CONSEQUENCE OF ECOLOGICAL INTERACTIONS

It is now time to revisit the definition of individual fitness used in this work. By definition of the dynamics (3), each organism merely pursues its own “selfish interest” in the environment where it happens to be. In each instance of “community competition” assayed in Fig. 4, whenever some species invaded a community, it was because its fitness in *that particular environment* was higher than the fitness of species already present. One could therefore argue that the surprising finding of Fig. 4, namely that the competition outcome is better predicted by collective, rather than individual, fitness is entirely a consequence of the unsatisfactory definition of individual fitness that sought to attribute a number to a genotype irrespective of its environment (Ribeck & Lenski 2015).

This observation is, of course, correct. However, from a practical standpoint, we do not typically have access to the exact conditions of the microenvironment experienced by any organism, and the definition (4) corresponds to how we might experimentally measure fitness, by placing an organism in a “typical” environment it is believed to experience. In the model described here, this typical environment is often an excellent approximation: for a community at equilibrium with equiabundant substrates $R_i = R$, the total community-wide expression of each pathway is roughly $T \simeq R/\chi_0$, the same for all i . Nevertheless, the minute deviations are sufficient to cause discrepancy between the true list of survivors and the prediction based on intrinsic fitness.

In an interacting community, context-dependent fitness and intrinsic fitness become decoupled (McIntire & Fajardo 2014; Ribeck & Lenski 2015). If the feedback from organisms onto their environment is sufficiently strong to induce substantial reordering of the relative fitness rank of different species, the context-dependent component of fitness may become dominant, and no measure of intrinsic fitness will remain a valid approximation. The model presented here highlights that this effect is an emergent phenomenon that stems from the ecological diversity of organisms in the community. It would not have been as apparent in the interactions of just two or three particular species, and would be obscured by the historic focus on pairwise interactions decoupled from their more complex community context (Hay *et al.* 2004; McGill *et al.* 2006).

If this interpretation of the origin of “fitness decoupling” observed in Fig. 4 is correct, then reducing the degree to which environmental perturbations affect rela-

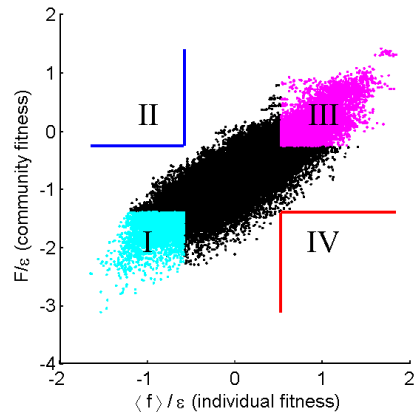


FIG. 5. **Parameter ϵ tunes the magnitude of fitness decoupling.** Same as Fig. 4A, for larger $\epsilon = 0.1$. Increasing ϵ reduces the relative importance of environment in determining the fitness ranking of species. As a result, collective and individual fitness remain strongly coupled. Defining quadrants as in Fig. 4A leaves the blue and red quadrants empty.

tive fitness of individuals should make fitness decoupling less pronounced. This prediction can be tested by increasing ϵ , the parameter that determines the width of the distribution of organism costs. For example, consider a community where the substrate A is disputed by only two organisms: \underline{A} and \underline{AB} . Assume that $f_{AB} > f_A$, so that when substrates A and B are equally abundant, the species \underline{AB} is more fit and displaces \underline{A} . Reducing the availability of substrate A can reverse this outcome (if A is absent, \underline{AB} can still survive, but not \underline{A}). However, the larger the difference in intrinsic fitness f_{AB} and f_A , the more extreme such resource depletion would have to be. Therefore, increasing ϵ will reduce the relative effect that changing environment has on fitness rank ordering. Fig. 5 repeats the analysis of Fig. 4A for $\epsilon = 0.1$ (rather than $\epsilon = 10^{-3}$ used previously). As predicted, the collective fitness is now strongly associated with the fitness of individuals. In fact, this is already apparent in Fig. 2B: as ϵ is increased, the median fitness rank of survivors at the final equilibrium begins to reduce. At high ϵ , it is increasingly true that high collective fitness is merely a reflection of high individual fitness of community members. Thus Fig. 2B documents a transition between a largely individualistic regime (at large ϵ) and a regime where the genetically inhomogenous assembly of species increasingly acts “as a whole”, in a rigorous mathematical, rather than purely metaphorical sense. Importantly, here the community-level description is appropriate not because of any explicit cooperation between members, but because the community is the smallest unit whose environment is well-defined and fixed (the resource influx \vec{R}). It is a consequence of the “experimental setup” (Swenson *et al.* 2000ab) where communities are allowed to evolve independently and interact through community-level coalescence events (a setting that, as emphasized

by Wilson, promotes group-level traits; Wilson 1977).

VI. DISCUSSION

It is intriguing to speculate that the argument presented here could be related to fitness decoupling occurring in major evolutionary transitions (Maynard Smith & Szathmary 1995, Calcott *et al.* 2011), whereupon the fitness of the group becomes distinct from the simple average of the fitness of its members (Michod 1999; Michod & Nedelcu 2003; Hammerschmidt *et al.* 2014). The results presented here link this puzzling phenomenon to the well-understood notion of context-dependent fitness, usually considered to be a rather separate issue. However, unlike this work, discussions of major evolutionary transitions operate with a reproductive definition of fitness (the canonical example being the germ/soma reproductive specialization in a multicellular organism; Michod 1999; Okasha 2008). Although coalescence can be seen as a form of community reproduction, exploring this parallel will require extending this approach to include reproduction of communities in a more formal manner.

In the particular model considered here, the community-wide dynamics took the form of optimizing a global “community fitness”. This feature made it easier to demonstrate how environment-dependent individual fitness translates into selection effectively acting on collective traits, e.g. favoring more efficient alliances of co-evolved organisms. In general, of course, collective dynamics are almost never reducible to optimizing one

global function (Metz *et al.* 2008), and one does not expect community to possess a well-defined “fitness”. However, the same could be said about the fitness of individual organisms. The traits possessed by organisms and correlated with their survival only translate into a fitness under some very specific circumstances when the environment is sufficiently stable and is sufficiently clearly demarcated from the system (“individuality”; Michod & Nedelcu 2003; Okasha 2008; Buss 1987). Such circumstances can arise via artificial selection in the hands of an experimenter imposing a standardized performance test (Swenson *et al.* 2000ab), or as a consequence of evolution, e.g. a pitcher plant or a host animal with its symbiont organisms; it seems likely that the conditions experienced by the symbionts themselves are not in this class. If whole-community coalescence events are indeed a significant factor shaping the evolutionary history of microbial consortia, then community-level functional integration of the type described here can be expected to be broadly relevant for natural communities (Doolittle & Zhaxybayeva 2010).

VII. ACKNOWLEDGMENTS

I thank Ariel Amir, Michael P. Brenner, Jeff Gore, Miriam H. Huntley, Simon A. Levin, Anne Pringle, Ned S. Wingreen and David Zwicker for helpful discussions, and anonymous referees for their comments on the early version of the manuscript. This work was supported by the Harvard Center of Mathematical Sciences and Applications, and the Simons Foundation.

-
- [1] Bakken, J.S., Borody, T., Brandt, L.J., Brill, J.V., Demarco, D.C., Franzos, M.A. et al. (2011). Treating *Clostridium difficile* Infection With Fecal Microbiota Transplantation. *Clin Gastroenterol H*, 9, 1044-1049.
 - [2] Birch, L.C. (1953). Experimental Background to the Study of the Distribution and Abundance of Insects .3. The Relation between Innate Capacity for Increase and Survival of Different Species of Beetles Living Together on the Same Food. *Evolution*, 7, 136-144.
 - [3] Buss, L.W. (1987). *The evolution of individuality*. Princeton University Press, Princeton, N.J.
 - [4] Calcott, B., Sterelny, K. & Szathmary, E.R. (2011). *The major transitions in evolution revisited*. MIT Press, Cambridge, Mass.
 - [5] Davis, A.J., Lawton, J.H., Shorrocks, B. & Jenkinson, L.S. (1998). Individualistic species responses invalidate simple physiological models of community dynamics under global environmental change. *J Anim Ecol*, 67, 600-612.
 - [6] Doolittle, W.F. and Zhaxybayeva, O. (2010). Metagenomics and the Units of Biological Organization. *Bio-science*, 60, 102-112.
 - [7] Geritz, S.A.H., Kisdi, E., Meszner, G. & Metz, J.A.J. (1998). Evolutionarily singular strategies and the adaptive growth and branching of the evolutionary tree. *Evol Ecol*, 12, 35-57.
 - [8] Hammerschmidt, K., Rose, C.J., Kerr, B. & Rainey, P.B. (2014). Life cycles, fitness decoupling and the evolution of multicellularity. *Nature*, 515, 75-+.
 - [9] Hay, M.E., Parker, J.D., Burkepile, D.E., Caudill, C.C., Wilson, A.E., Hallinan, Z.P. et al. (2004). Mutualisms and aquatic community structure: The enemy of my enemy is my friend. *Annu Rev Ecol Evol Syst*, 35, 175-197.
 - [10] Kort, R., Caspers, M., van de Graaf, A., van Egmond, W., Keijser, B. & Roeselers, G. (2014). Shaping the oral microbiota through intimate kissing. *Microbiome*, 2.
 - [11] Levin, S.A., Segel, L.A. & Adler, F.R. (1990). Diffuse Coevolution in Plant-Herbivore Communities. *Theor Popul Biol*, 37, 171-191.
 - [12] Levin, S.R., Brock, D.A., Queller, D.C. & Strassmann, J.E. (2015). Concurrent coevolution of intra-organismal cheaters and resisters. *J Evol Biol*, 28, 756-765.
 - [13] MacArthur, R. (1969). Species Packing, and What Interspecies Competition Minimizes. *Proc Natl Acad Sci U S A*, 64, 1369-&.
 - [14] Maynard Smith, J. and Szathmary, E.R. (1995). *The major transitions in evolution*. W.H. Freeman Spektrum, Oxford ; New York.

- [15] McGill, B.J., Enquist, B.J., Weiher, E. and Westoby, M. (2006). Rebuilding community ecology from functional traits. *Trends Ecol Evol*, 21, 178-185.
- [16] McIntire, E.J.B. and Fajardo, A. (2014). Facilitation as a ubiquitous driver of biodiversity. *New Phytol*, 201, 403-416.
- [17] Metz, J.A.J., Mylius, S.D. and Diekmann, O. (2008). When does evolution optimize? *Evol Ecol Res*, 10, 629-654.
- [18] Michod, R.E. (1999). *Darwinian dynamics : evolutionary transitions in fitness and individuality*. Princeton University Press, Princeton, N.J.
- [19] Michod, R.E. and Nedelcu, A.M. (2003). On the reorganization of fitness during evolutionary transitions in individuality. *Integr Comp Biol*, 43, 64-73.
- [20] Moreno, E. and Rhiner, C. (2014). Darwin's multicellularity: from neurotrophic theories and cell competition to fitness fingerprints. *Curr Opin Cell Biol*, 31, 16-22.
- [21] Nurmi, T. and Parvinen, K. (2008). On the evolution of specialization with a mechanistic underpinning in structured metapopulations. *Theor Popul Biol*, 73, 222-243.
- [22] Okasha, S. (2008). *Evolution and the levels of selection*. Clarendon Press ; Oxford University Press, Oxford.
- [23] Qin, N., Yang, F.L., Li, A., Prifti, E., Chen, Y.F., Shao, L. et al. (2014). Alterations of the human gut microbiome in liver cirrhosis. *Nature*, 513, 59-+.
- [24] Queller, D.C. (2000). Relatedness and the fraternal major transitions. *Philos T Roy Soc B*, 355, 1647-1655.
- [25] Queller, D.C. and Strassmann, J.E. (2009). Beyond society: the evolution of organismality. *Philos T R Soc B*, 364, 3143-3155.
- [26] Ribeck, N. and Lenski, R.E. (2015). Modeling and quantifying frequency-dependent fitness in microbial populations with cross-feeding interactions. *Evolution*, 69, 1313-1320.
- [27] Ridaura, V.K., Faith, J.J., Rey, F.E., Cheng, J.Y., Duncan, A.E., Kau, A.L. et al. (2013). Gut Microbiota from Twins Discordant for Obesity Modulate Metabolism in Mice. *Science*, 341, 1079-U1049.
- [28] Rillig, M.C., Antonovics, J., Caruso, T., Lehmann, A., Powell, J.R., Veresoglou, S.D. et al. (2015). Interchange of entire communities: microbial community coalescence. *Trends Ecol Evol*, 30, 470-476.
- [29] Rosen, M.J., Davison, M., Bhaya, D. and Fisher, D.S. (2015). Fine-scale diversity and extensive recombination in a quasisexual bacterial population occupying a broad niche. *Science*, 348, 1019-1023.
- [30] Roughgarden, J. (1976). Resource Partitioning among Competing Species - Co-Evolutionary Approach. *Theor Popul Biol*, 9, 388-424.
- [31] Shapiro, B.J., Friedman, J., Cordero, O.X., Preheim, S.P., Timberlake, S.C., Szabo, G. et al. (2012). Population Genomics of Early Events in the Ecological Differentiation of Bacteria. *Science*, 336, 48-51.
- [32] Shapiro, J.A. (1998). Thinking about bacterial populations as multicellular organisms. *Annu Rev Microbiol*, 52, 81-104.
- [33] Slatkin, M. and Wilson, D.S. (1979). Coevolution in Structured Demes. *Proc Natl Acad Sci U S A*, 76, 2084-2087.
- [34] Swenson, W., Arendt, J. & Wilson, D.S. (2000). Artificial selection of microbial ecosystems for 3-chloroaniline biodegradation. *Environ Microbiol*, 2, 564-571.
- [35] Swenson, W., Wilson, D.S. and Elias, R. (2000). Artificial ecosystem selection. *Proc Natl Acad Sci U S A*, 97, 9110-9114.
- [36] Tilman, D. (1990). Constraints and Tradeoffs - toward a Predictive Theory of Competition and Succession. *Oikos*, 58, 3-15.
- [37] West, S.A., Griffin, A.S., Gardner, A. and Diggle, S.P. (2006). Social evolution theory for microorganisms. *Nat Rev Microbiol*, 4, 597-607.
- [38] Wilson, D.S. (1977). Structured Demes and Evolution of Group-Advantageous Traits. *Amer Nat*, 111, 157-185.

SUPPLEMENTARY MATERIAL

1. Relation to the model of MacArthur

The dynamics (3) can be written as

$$\frac{dn_{\vec{\sigma}}}{dt} = \frac{1}{\tau_0 |\chi_{\vec{\sigma}}|} n_{\vec{\sigma}} \left(\sum_i \sigma_i A_i - \chi_{\vec{\sigma}} \right). \quad (\text{S1})$$

where A_i denotes the ‘‘available resources’’. In the model considered in this work, $A_i = \frac{R_i}{T_i}$. MacArthur (1969) considered a model of species competing for renewing resources. In that model, the dynamics of organism populations were identical to (S1), but the availability of resources was given by $A_i = R_i(1 - T_i/r_i)$ (see equations (1)-(3) in MacArthur 1969), where the extra parameter r_i is the renewal rate (or the ‘‘intrinsic rate of natural increase’’).

The dynamics of the two models, therefore, differ only by the choice of the functional form relating population growth and the corresponding decrease of resource availability. The mapping between the notations of MacArthur 1969 (‘‘MA’’) and those used here is provided in the table:

Notation for...	MA	Here
Species index	i	$\vec{\sigma}$
Species abundance	x_i	$n_{\vec{\sigma}}$
Resources a species can harvest	a_{ij}	σ_i
Resource carrying capacity	K_j	R_i
Minimal resource requirement	T_i	$\chi_{\vec{\sigma}}$
‘‘Resource weight’’	w_i	1
Resources \mapsto biomass conversion factor	c_i	$(\tau_0 \chi_{\vec{\sigma}})^{-1}$
Resource renewal rate	r_j	N/A

In the work of MacArthur, each species i was described by an arbitrary chosen vector of parameters a_{ij} (probability to encounter and consume resource j). The space of possibilities is unconstrained, and the types available to form a community are fixed by historical contingency; MacArthur then asks how many species can co-exist in this way. In the model considered here, a_{ij} are constrained to be 0 or 1. The setting is treated as an adaptive dynamics model where species are allowed to acquire or lose pathways, and the outcome of this co-evolution is investigated.

Reformulating community dynamics as an optimization problem was first done in MacArthur 1969; here, because of the difference in the way resource consumption is treated, the objective function being optimized is different, but the argument is similar. Consider the following objective function:

$$\tilde{F} = \sum_i R_i \ln T_i - \sum_{\vec{\sigma}} \chi_{\vec{\sigma}} n_{\vec{\sigma}}, \quad (\text{S2})$$

defined for $\{n_{\vec{\sigma}} \geq 0\}$, and differing from the definition of Eq. (5) only by normalization.

\tilde{F} is bounded from above. To see this, note the inequalities:

$$\sum_i T_i = \sum_{\vec{\sigma}} |\vec{\sigma}| n_{\vec{\sigma}} \leq N \sum_{\vec{\sigma}} n_{\vec{\sigma}}$$

and for $\alpha, \beta > 0$:

$$\alpha \ln x - \beta x \leq \alpha \ln \frac{\alpha}{e\beta}$$

Using these, and setting $\min_{\vec{\sigma}} \chi_{\vec{\sigma}} = \chi^* > 0$, one can write:

$$\begin{aligned} \tilde{F} &\leq \sum_i R_i \ln T_i - \chi^* \sum_{\vec{\sigma}} n_{\vec{\sigma}} \leq \sum_i \left(R_i \ln T_i - \frac{\chi^*}{N} T_i \right) \\ &\leq \sum_i R_i \ln \frac{NR_i}{e\chi^*} \end{aligned}$$

\tilde{F} is convex. To see this, note that for any function $f(\vec{n})$, the following two operations leave its convexity invariant (M is an arbitrary matrix):

1. adding a linear function of its arguments:

$$f(\vec{n}) \mapsto g(\vec{n}) = f(\vec{n}) + M\vec{n};$$

2. performing a linear transformation of its arguments:

$$f(\vec{n}) \mapsto h(\vec{n}) = f(M\vec{n}).$$

Given these observations, convexity of \tilde{F} , and therefore also the convexity of F as defined in (5), directly follows from the convexity of the logarithm.

The main text demonstrated that \tilde{F} is always increasing along the trajectories of the model. Thus, for any initial community state \mathcal{C} , ecological dynamics converge to the equilibrium corresponding to the unique maximum of \tilde{F} on the domain $\{n_{\vec{\sigma}} \geq 0 \text{ for } \vec{\sigma} \in \Omega(\mathcal{C})\}$. Since \tilde{F} is bounded and convex, the final equilibrium always exists and is unique and stable.

2. Normalization of community fitness

The typical value of \tilde{F} as defined in equation (S2) for a community close to equilibrium can be estimated as follows.

To estimate the first term, note that the cost per pathway of all organisms is close to χ_0 , and therefore the overall expression T_i is approximately $T_i \approx R_i/\chi_0$.

The second term is the total cost of all organisms in the population $\sum_{\vec{\sigma}} n_{\vec{\sigma}} \chi_{\vec{\sigma}}$. At any equilibrium, it is equal to the total resource abundance $R_{\text{tot}} \equiv \sum_i R_i$. This can be seen in two ways. One approach is to use the equilibria

conditions to express the cost of all present organisms in terms of resources:

$$\forall \vec{\sigma} \in \Omega(\mathcal{C}): \chi_{\vec{\sigma}} = \sum_i \sigma_i \frac{R_i}{T_i}$$

Therefore,

$$\sum_{\vec{\sigma}} n_{\vec{\sigma}} \chi_{\vec{\sigma}} = \sum_i \left(\sum_{\vec{\sigma}} n_{\vec{\sigma}} \sigma_i \right) \frac{R_i}{T_i} = \sum_i R_i.$$

Alternatively, this same equation can be derived from the condition of maximization of \tilde{F} , by setting $n_{\vec{\sigma}} \equiv Mp_{\vec{\sigma}}$, and requiring $\frac{\partial \tilde{F}}{\partial M} = 0$.

Putting these observations together, the expectation for the value of \tilde{F} at any equilibrium is therefore

$$\begin{aligned} \tilde{F} &= \sum_i R_i \ln T_i - \sum_{\vec{\sigma}} \chi_{\vec{\sigma}} n_{\vec{\sigma}} = \sum_i R_i \ln T_i - \sum_i R_i \\ &\approx \sum_i R_i \ln(R_i/\chi_0) - \sum_i R_i \equiv \tilde{F}_0 \quad (\text{S3}) \end{aligned}$$

When defining community fitness, it is natural to subtract this baseline value from \tilde{F} as defined in (S2), and normalize by R_{tot} :

$$F = \frac{\tilde{F} - \tilde{F}_0}{\sum_i R_i}.$$

This is the normalization chosen in equation (5) in the main text.

3. Sensitivity to the value of ϵ

Fig. 2B demonstrates that for small enough ϵ , the structure of the final equilibria does not significantly depend on this parameter. This can be intuitively understood as follows. Consider two resources A, B and organisms $\underline{A} = \{1, 0\}$, $\underline{B} = \{0, 1\}$, and $\underline{AB} = \{1, 1\}$. If

$$\chi_{\underline{AB}} > \chi_{\underline{A}} + \chi_{\underline{B}}, \quad (\text{S4})$$

it easily follows that the ‘‘generalist’’ organism \underline{AB} will eventually be outcompeted by the two specialists \underline{A} and \underline{B} . Conversely, if the opposite inequality holds, then \underline{A} and \underline{B} cannot stably coexist in the final equilibrium, since \underline{AB} will always be able to invade, displacing one (or both) of them. In this way, in the metagenome partitioning model, community composition is shaped primarily by inequalities like (S4), which are invariant under changes in ϵ and depend only on the realization of the ‘‘noise’’ ξ .

4. The maximum number of coexisting types

The traditional question of how many types can coexist for a given set of parameters, although not at the focus of

this work, is nevertheless instructive to address. A simple linear algebra argument demonstrates that in the model considered here, this maximum number is N : a stable coexistence is possible only for a number of types that is at most equal to the number of resources. This is because for a given set of K types, the K equilibria conditions $\Delta\varphi_{\vec{\sigma}} = 0$ can be seen as a linear mapping between the N -dimensional vector R_i/T_i and a K -dimensional vector of organism costs $\chi_{\vec{\sigma}}$. In the generic case (i.e. if no special symmetries exist in the cost structure), the existence of such a mapping requires $K \leq N$.

Symmetries in the cost structure can lead to degenerate equilibria circumventing this maximal coexistence condition. Imagine, for example, that all organisms have the exact same cost per pathway χ^* . In this maximally degenerate case *any* combination of functional types can coexist, provided that $T_i = R_i/\chi^*$: no division of labor strategy is better than any other.

5. Numerical determination of community equilibrium

To determine the equilibrium state established through competition of a given set of K species, one could imagine choosing a random starting point with a non-vanishing abundance of all K competing species, and evolving it according to the dynamical equations for time $t \rightarrow \infty$. The Lyapunov function guarantees that such evolution would converge to an equilibrium state. However, if $K \gg N$ (for example, $K = 1023$ and $N = 10$ in Fig. 2A), such a procedure is highly memory-intensive and wasteful, since the final population is guaranteed to contain at most N types with non-zero abundance (see section ‘‘The maximum number of coexisting types’’).

Conveniently, verifying that a configuration is a final equilibrium is much easier than finding it: one only needs to check that the resource surplus $\Delta\varphi_{\vec{\sigma}}$ is zero for all competitors that survived and is negative for all those who went extinct. This verification is fast and is guaranteed to either confirm that the equilibrium state is correct, or provide a list of species that can invade it. Therefore, a simple heuristic procedure can construct the true equilibrium configuration through an iterated sequence of ‘‘guesses’’, whereby a subset of species is first equilibrated, and then updated by removing species that went extinct and adding those that can invade. This is the approach adopted here.

Specifically, calculations were performed in Matlab (Mathworks, Inc.). Availability of all resources was set to $R = 100$. The ‘‘initial guess’’ S_0 is constructed using the individual fitness criterion explained in the main text (low cost per pathway = high fitness): for each pathway i , the 10 most cost-efficient (lowest cost per pathway) functional types ($S_0^{(i)}$) that contained pathway i are determined; the union of these cost-efficient types, all taken at equal abundance of 1 unit, constitutes the ‘‘initial guess’’ $S_0 = \bigcup_i S_0^{(i)}$.

The following procedure is then iterated: community dynamics are simulated using MatLab’s variable-order differential equation solver `ode15s` until the absolute magnitude of all time derivatives $\dot{n}_{\bar{\sigma}}$ fall below threshold $10^{-4}\epsilon$. At this point, most of the very-low-abundance species still present in the community are in the process of exponential extinction. To ensure that all such low-abundance types are indeed going extinct, all types with abundance below 10^{-4} are removed from the population, the pruned community is re-equilibrated (to account for any tiny adjustments this removal might have caused), and the resulting state \mathcal{C}^* is tested for being a non-invadable equilibrium. If any invaders are found, they are added to the community at abundance 1, and the simulation cycle is repeated. Otherwise (no species can invade), the configuration is accepted as being within the pre-determined numerical error of the true final equilibrium. This protocol ensures that in the community \mathcal{C}^* , the list of survivors is exact (because the invadability criterion is always checked for all competing species and is exact), and their abundance is within acceptable numerical error. The protocol always converged due to convexity of “community fitness” F .

Scripts performing calculations and reproducing Figs. 2–5 are available as Supplementary File 1.

Appendix A: Supplementary information for Figure 2B

Figure 2B was generated as follows. For a given cost structure, 10 random subsets Ω_i of 100 types each were equilibrated to determine survivors S_i^* . The procedure was repeated for 10 random realizations of the cost structure at each ϵ , with ϵ ranging from 10^{-5} to 0.1. Thus for each value of ϵ , a total of 100 randomly constructed communities were evaluated. Fig. 2B shows the median fitness rank of survivors S^* within the respective set of competitors, averaged over all 100 instances, where the median was either weighted (blue dashed line) or not weighted (red solid line) by abundance of the type at equilibrium.

Appendix B: Initial conditions for Fig. 3

The trajectories displayed in Fig. 3 were simulated for time $T = 10^6$ starting from 10 random initial conditions whereby each of the 1023 types was set to an abundance value drawn out of a log-uniform distribution between 10^{-5} and 100.